

**Smart Rock Technology for Real-time Monitoring of Bridge Scour
and Riprap Effectiveness – Design Guidelines and Visualization Tools
(Progress Report No. 7)**

**Contract No: OASRTRS-14-H-MST
(Missouri University of Science and Technology)**

Reporting Period: April 1 – June 31, 2015

PI: Genda Chen

Program Manager: Mr. Caesar Singh

Submission Date: July 15, 2016

TABLE OF CONTENTS

EXECUTIVE SUMMARY	1
I - TECHNICAL STATUS.....	2
I.1 ACCOMPLISHMENTS BY MILESTONE.....	2
<i>Task 3.1 Time- and Event-based Field Measurements</i>	<i>2</i>
<i>Task 3.2 Visualization Tools for Rock Location Mapping over Time.....</i>	<i>10</i>
<i>Task 4 Technology Transfer, Report and Travel Requirements</i>	<i>10</i>
I.2 PROBLEMS ENCOUNTERED.....	10
I.3 FUTURE PLAN	10
<i>Task 3.1 Time- and Event-based Field Measurements</i>	<i>10</i>
<i>Task 3.2 Visualization Tools for Rock Location Mapping over Time.....</i>	<i>11</i>
<i>Task 4 Technology Transfer, Report and Travel Requirements</i>	<i>11</i>
II – BUSINESS STATUS	12
II.1 HOURS/EFFORT EXPENDED	12
II.2 FUNDS EXPENDED AND COST SHARE.....	13

EXECUTIVE SUMMARY

During the 7th quarter of this project, the 2nd field demonstration tests were carried out at the I-44W Bridge (No. L0093) over the Roubidoux Creek in Missouri. This report summarizes the test results and findings.

I - TECHNICAL STATUS

I.1 ACCOMPLISHMENTS BY MILESTONE

In this quarter, another series of field tests were carried out at the I-44W Roubidoux Creek Bridge, Br. No, L0039, MO. One smart rock with two N42 magnets stacked and set in an automatically pointing-up system (APUS) was deployed at the downstream of Bent 7 during the first series of field tests as described in Report No.5. The second tests aimed at checking if the smart rock had been moved to the deepest point in a scour hole. The smart rock was located from the measurements taken with the test crane set at the same locations on the bridge deck as used during the first test. The 3-axis flux magnetometer sensor head and a nearby prism were mounted on the test crane. The sensor head was used to measure the magnetic field and the prism was used as a target to survey the coordinates of each measurement point. Finally, the new position of the smart rock was located based on the magnetic field data and measurement point coordinates.

Task 3.1 Time- and Event-based Field Measurements

In this task, field tests were carried out on the deck of I-44W Roubidoux Creek Bridge as shown in Figure 1. First, the smart rock deployed previously at the downstream of Bent 7 was physically located by a diver as a ground true data for the rock localization algorithm and a confirmation that it was rolled to the bottom of the scour hole. Then, the rock was mathematically located from field measurements taken following the same procedure as used during the first series of field tests. For this series of tests, the smart rock was already in place so that only the total magnetic field around the smart rock was measured. For the ambient magnetic field, Bent 5 far away from the smart rock was selected as a reference. Five permanent points near Bent 5 were selected to investigate the variation of the ambient magnetic field over time. Another point far away from the bridge Bent 5 was chosen as the permanent point to investigate the variation of the Earth magnetic field.

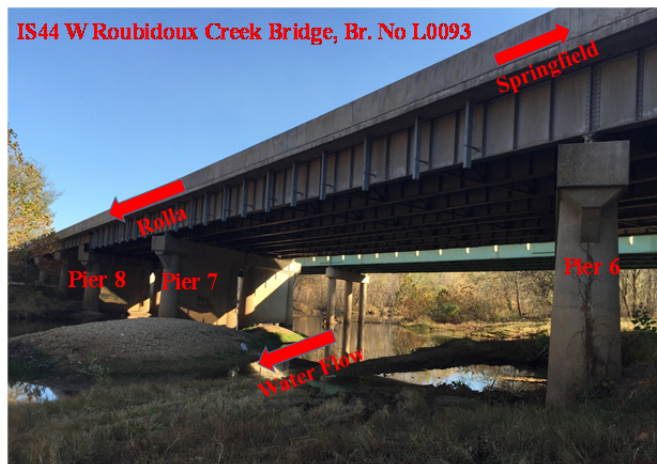
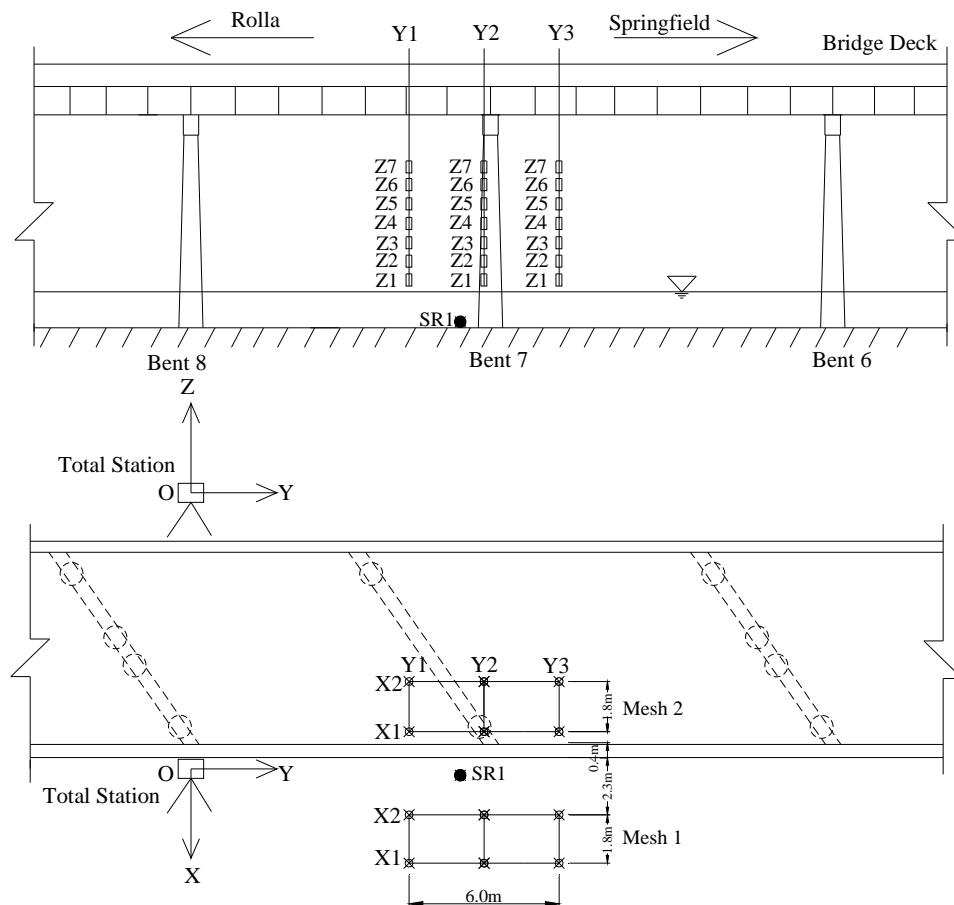


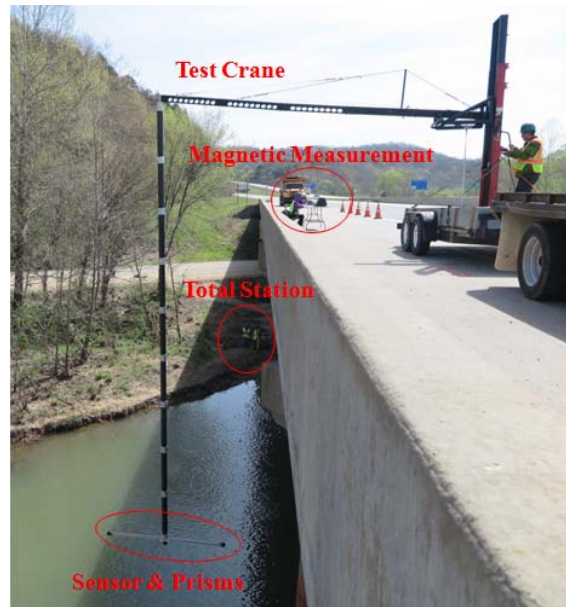
Figure 1 I-44W Roubidoux Creek Bridge

A. Test Setup and Layout

All tests were conducted on the bridge shoulder near Bent 7 as shown in Figure 2(a, b). A total station was set near Bent 8. Its position was used as the origin of a Cartesian coordinate system XYZ with X-, Y-, and Z-axes oriented in transverse, longitudinal (traffic direction), and vertical (upward) directions, respectively. The smart rock, SR1, was confirmed around Bent 7. The test crane was fixed on a trailer towed by a truck. The magnetometer sensor mounted on the test crane was extended down from the bridge deck to measure the total magnetic field near the smart rock. Prism 3 mounted below the sensor as shown in Figure 2(c) was used to represent the coordinate of each measurement point. Prisms 1 and 2 fixed at two ends of the horizontal bar of the test crane were employed to ensure that the horizontal bar was in parallel with X axis. The measurement points, as shown in Figure 2(a), are exactly the same locations as used during the first series of field tests. The sensor points were translated to the corresponding forklift locations on the bridge deck, as displayed in Figure 2(d). For each point in XOY plane, seven elevations denoted as Z1, Z2, Z3, Z4, Z5, Z6 and Z7 with equal spacing of 0.3 m were considered for measurements in Z-direction. The total station set near Bent 8 was used to survey the coordinates (location) of the smart rock and magnetometer sensor as ground true data.



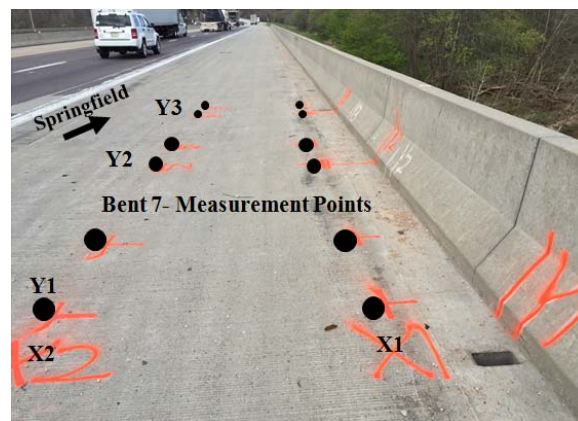
(a) Schematic View of Smart Rock and Sensor Locations in Plane



(b) Layout of the Overall Measurement System



(c) Sensor and Prisms Positions



(d) Measurement Points Arrangement on Bridge Deck
 Figure 2 Test Setup at I-44W Roubidoux Creek Bridge Site

B. Test Procedures

(1) **Set the XYZ Coordinate System.** As shown in Figure 3, a proper location for the total station was selected near Bent 8 for its line of sight to the magnetometer sensor, which is designated as Point O or the origin of the coordinate system. The Y-axis pointing to Springfield was selected to be the longitudinal (traffic) direction of the straight bridge deck, passing through Point O. The X-axis is perpendicular to the Y-axis and pointing to downstream in the horizontal plane, and the Z-axis is upward according to the right hand rule. A permanent point A (Benchmark) on Pier 9 was also surveyed for future reference and translation from the measurement points under O-XYZ to the coordinates selected during the first series of field tests. Based on the two tests conducted thus far, the difference between the origins of the two coordinate systems is very small.

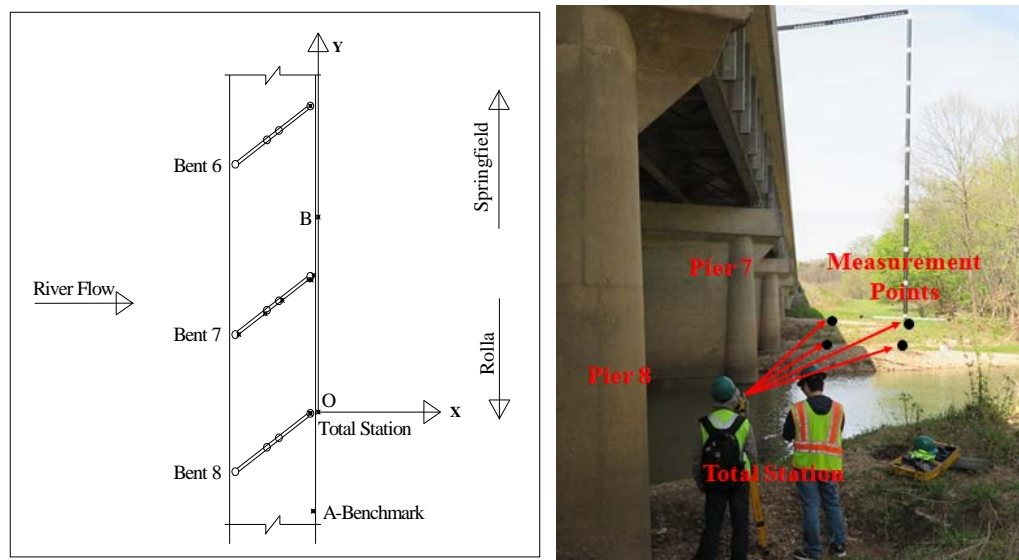


Figure 3 Selection of the Cartesian Coordinate System

(2) **Assemble the Test Crane.** As shown in Figures 2(b), the forklift was first set and tied to an open trailer. The horizontal aluminum arm was then installed and followed by an assembling of nine segments of carbon fiber tubes with 1.0 meter each to lower down the measurement points from the bridge deck. Finally, the horizontal bar was connected at the bottom of the carbon tube to support the magnetometer sensor and prisms for coordinate measurement.

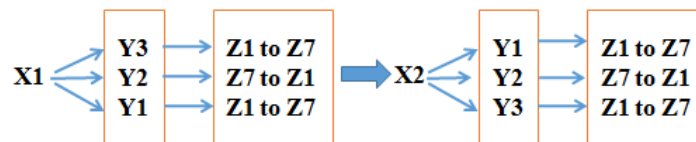
(3) **Set up the STL Digital Magnetometer.** As shown in Figure 2(b), the laptop installed with special software for the sensor controls the measurement of magnetic fields. An Ethernet cable was used to transmit the signal from the sensor to the laptop by an interface called mini Ethernet box. Two batteries were used to power the sensor and laptop.

(4) **Measure the Total Magnetic Field.** The total magnetic field is a combination of the effects of the smart rock, the Earth, and the bridge environment. As indicated in Figure 2(a, b, d), the

trailer ran two paths (X coordinates) on the bridge deck and three stops (Y coordinates). At each stop, seven elevations (Z coordinates) were selected by moving up and down the horizontal arm of the test crane by 0.3 m as used during the first series of field tests. Figure 4(a) illustrates one stop when the two rear tires of the trailer were parked at the marked location and the forklift was positioned at X2Y3. At each stop, seven measurements (both coordinate and magnetic field intensity) were taken at seven elevations. Therefore, a total of 42 measurements were taken as indicated in Figure 4(b).



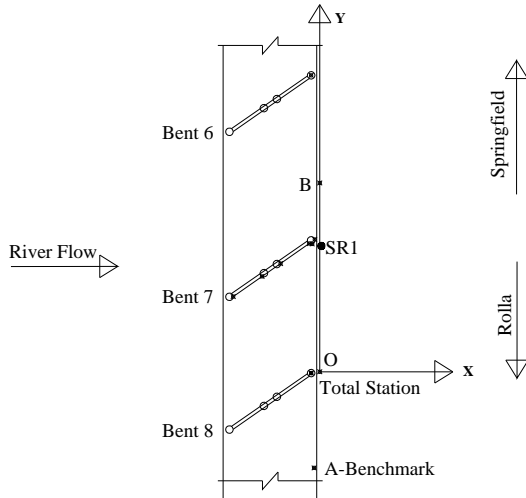
(a) Test Crane Located at Y2X2



(b) Measurement Point Sequence

Figure 4 Planning of the Total Magnetic Field Measurement

(5) *Inspect the Smart Rock and Measure its Coordinates.* The smart rock, SR1, was inspected to ensure that it was rolled to the bottom of the scour hole around Bent 7. It was found to have slightly moved from the original position when deployed during the first series of field tests. The coordinate of the smart rock in the new position was surveyed with a total station through the prism placed on top of the smart rock, which is used for ground truth data in smart rock localization. Figure 5 indicates the approximate location and the coordinate measurement of the inspected smart rock.



(a) Schematic View of SR1 Location



(b) Survey of SR1 Smart Rock

Figure 5 Coordinate Measurement of the Smart Rock

(6) **Measure the Ambient Magnetic Field (AMF) for Reference.** Bent 5 is approximately 61 m away from Bent 7. Pier 5 was thus selected as a reference site for a study of potential change of the ambient magnetic field over time. Five permanent points, P5-1, P5-2, P5-3, P5-4 and P5-5 as shown in Figure 6(a) were selected at the top of orange markers. The magnitude of the ambient magnetic field for each point was measured by a scalar magnetometer G858. Note that the magnetic intensity change over time, measured near Pier 5, can be used to understand any potential time-varying change of the ambient magnetic field near Bent 7. P5 area at least 15 m away from Pier 5, as circled in Figure 6(b), was selected during the first series of field tests as a reference location for the Earth magnetic field intensity. It was found that the intensity inside the P5 area changed little as observed during the first tests, indicating little influence from the bridge pier or deck and thus the Earth's magnetic field only. Continuing measurements in the P5 area shed light on any potential change of the Earth magnetic field between various field tests.

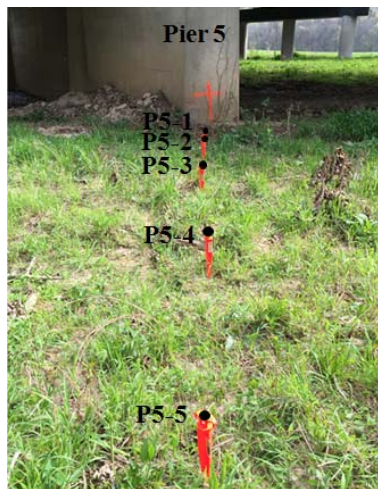


Figure 6 Ambient Magnetic Field Measurement near Pier 5

D. Localization Algorithm

The total magnetic field intensity (B) is a function of the ambient field (B_{XA} , B_{YA} and B_{ZA}) and the magnetic field of a smart rock at (X_M , Y_M , Z_M). Both the total and ambient magnetic fields were measured at each measurement point (X , Y , Z) so that an objective error function can be formulated and minimized to determine the location of the smart rock.

E. Test Results and Discussion

Table 1 summarizes the coordinates of 42 measurement points, the ambient magnetic field (AMF) intensities and the total magnetic field intensities. The coordinates presented in Table 1 have been transformed to the coordinate system set up during the first series of field tests as described in Report No. 5 through the benchmark point A surveyed at both series of field tests. The coordinate transformation is necessary to ensure that the movement of the smart rock can be illustrated under one coordinate system. The AMF is generated by the Earth and nearby ferromagnetic objects embedded in the bridge pier and deck. The effect from the bridge pier and deck on the AMF is stationary and time independent since the distribution of ferromagnetic materials in the pier and deck remains unchanged over time. However, the Earth magnetic field would vary over time in days, seasons or years as a result of the direct or indirect effect of solar wind. Therefore, the AMF measured prior to the initial deployment of the smart rock must be modified for the Earth effect.

Table 1 Coordinates and Magnetic Field Intensities at various Measurement Points

Measurement Point Coordinate (m)				Factor (nT.m ³)	AMF Intensity (nT)					
		X_i	Y_i	Z_i	k	B_{Ax}	B_{Ay}	B_{Az}	B_A	B
X1Y1	Z1	3.829	21.766	-1.004	86521	22940	1023	-49252	54342	53746
	Z2	3.817	21.662	-0.713	86521	22564	1754	-49347	54181	53850
	Z3	3.796	21.612	-0.411	86521	22575	2246	-49293	54155	53952
	Z4	3.804	21.647	-0.123	86521	22601	2387	-49255	54137	54035
	Z5	3.756	21.508	0.183	86521	22568	2337	-49249	54116	54089
	Z6	3.792	21.559	0.474	86521	23026	3368	-49014	54150	54157
	Z7	3.806	21.531	0.791	86521	22790	2415	-49119	54095	54187
X1Y2	Z1	3.832	24.537	-0.999	86521	22627	2177	-49075	53977	53181
	Z2	3.874	24.423	-0.744	86521	22713	2496	-48954	53917	53422
	Z3	3.796	24.397	-0.397	86521	22569	2561	-48961	53866	53605
	Z4	3.751	24.338	-0.130	86521	23043	2814	-48689	53833	53747
	Z5	3.818	24.374	0.188	86521	22523	2815	-48890	53795	53845
	Z6	3.778	24.342	0.470	86521	22636	2728	-48815	53770	53927
	Z7	3.751	24.231	0.773	86521	22506	2805	-48845	53746	53960
X1Y3	Z1	3.850	27.663	-1.018	86521	21640	2266	-49333	53811	53394
	Z2	3.844	27.618	-0.728	86521	21693	2419	-49289	53799	53474

	Z3	3.747	27.568	-0.424	86521	21727	2706	-49249	53790	53551
	Z4	3.838	27.501	-0.119	86521	21898	2543	-49177	53785	53619
	Z5	3.853	27.577	0.191	86521	22012	2761	-49074	53748	53674
	Z6	3.826	27.538	0.470	86521	21929	2602	-49124	53752	53719
	Z7	3.849	27.493	0.773	86521	21913	3415	-49030	53706	53742
X2Y1	Z1	2.054	21.861	-0.999	86521	22935	1678	-49275	54269	54047
	Z2	2.066	21.715	-0.723	86521	22935	1678	-49275	54269	54334
	Z3	2.063	21.878	-0.423	86521	22614	2814	-49454	54344	54557
	Z4	2.076	21.678	-0.113	86521	22609	2884	-49526	54410	54756
	Z5	2.070	21.617	0.194	86521	22559	2730	-49637	54482	54925
	Z6	2.059	21.612	0.473	86521	22614	2955	-49728	54600	55089
	Z7	2.068	21.619	0.775	86521	22653	3260	-49823	54720	55217
X2Y2	Z1	2.074	24.548	-0.993	86521	23109	4441	-48319	53638	55899
	Z2	2.010	24.412	-0.714	86521	23007	4968	-48183	53518	55802
	Z3	2.074	24.433	-0.411	86521	22836	5724	-48144	53485	55706
	Z4	2.078	24.455	-0.112	86521	22489	5271	-48526	53636	55599
	Z5	2.089	24.467	0.196	86521	22485	4990	-48711	53775	55470
	Z6	2.092	24.203	0.487	86521	22392	5231	-48895	53925	55440
	Z7	2.086	24.321	0.791	86521	22452	5588	-49000	54081	55394
X2Y3	Z1	2.135	27.568	-1.012	86521	20988	5262	-49629	54034	53723
	Z2	2.133	27.316	-0.717	86521	21036	5322	-49617	54046	53923
	Z3	2.062	27.230	-0.403	86521	21225	5488	-49548	54074	54113
	Z4	2.041	27.370	-0.120	86521	21197	5411	-49618	54119	54265
	Z5	2.049	27.250	0.184	86521	21428	5397	-49594	54186	54424
	Z6	2.110	27.306	0.470	86521	21684	5833	-49467	54218	54545
	Z7	2.035	27.279	0.763	86521	21851	6926	-49317	54276	54668

During the second series of field tests as discussed in this report, the ambient magnetic intensity in the P5 area measured with the magnetometer G858 is 52123 nT, which is different from 51761 nT that was measured during the first series of field tests as described in Report No. 5. It can be seen that the Earth magnetic field intensity is increased by 0.7% with respect to the first series of field tests. Since the two O-XYZ coordinate systems used during the first and second series of field tests are identical except with different origins and the direction of the Earth magnetic field is assumed to remain unchanged over time, the change in three components of the Earth magnetic field is proportional to that in magnitude of the Earth field. Knowing the direction of the Earth magnetic field, each component of the AMF in Report No. 5 can be increased by an amount equal to the product of (52123-51761) and the cosine coefficient. The modified AMF is presented in Table 1.

The coefficient k for two stacked N42 magnets was calculated from the maximum residual flux density. The three components of the total magnetic field (B_x, B_y, B_z) were directly measured with the 3-axis flux magnetometer that was oriented in parallel with the O-XYZ coordinate system. Therefore, the three components of the total magnetic field and the three components (B_{Ax}, B_{Ay} and B_{Az}) of the ambient magnetic field were substituted into the localization algorithm to determine the coordinates of the smart rock SR1.

Table 2 compares the predicted and measured coordinates (X_M, Y_M, Z_M) of the smart rock SR1. It was calculated from the measured coordinates and magnetic intensities at various sensor locations. The overall error is 0.333 m, which is less than the error limit of 0.5 m set forth at the beginning of this project. Therefore, the analysis method to account for a variation of the ambient magnetic field over time is acceptable for bridge scour monitoring with smart rocks.

Table 2 Predicted and Measured Location of SR1

Parameter	X_M (m)	Y_M (m)	Z_M (m)
Predicted SR1 Location	0.554	24.384	-3.214
Measured SR1 Location	0.366	24.601	-3.382
Location Prediction Error in Coordinate	0.188	-0.217	0.168
SRSS Error in Rock Location	0.333 m		

Task 3.2 Visualization Tools for Rock Location Mapping over Time

Tests for the mapping of the river bed profile around Bent 7 of the I-44W Roubidoux Creek Bridge were completed using a side imaging instrument. The data processing and visualization of the movement of the smart rock SR1 are currently on going and will be documented in the final report.

Task 4 Technology Transfer, Report and Travel Requirements

The 7th quarterly report is being submitted.

I.2 PROBLEMS ENCOUNTERED

In this quarter, additional field tests were delayed since the field experienced specialist went through a surgeon that requires about two months of sick leave.

I.3 FUTURE PLAN

The following task and subtasks will be executed during the next quarter.

Task 3.1 Time- and Event-based Field Measurements

The field tests at one bridge in California and two bridge sites in Missouri will continue to further validate the movement and localization of smart rocks.

Task 3.2 Visualization Tools for Rock Location Mapping over Time

This task will be completed based on the field tests at the bridge sites in California and Missouri.

Task 4 Technology Transfer, Report and Travel Requirements

The 8th quarterly report will be prepared and submitted.

.

II – BUSINESS STATUS

II.1 HOURS/EFFORT EXPENDED

The planned hours and the actual hours spent on this project are given and compared in Table 3. In the seventh quarter, the actual hours spent are less than the planned hours, leading to an actual cumulative hour of approximately 110% of the planned hours. The cumulative hours spent on various tasks by personnel are presented in Figure 7.

Table 3 Hours Spent on This Project

	Planned		Actual	
	Labor Hours	Cumulative	Labor Hours	Cumulative
Quarter 1	236	236	176	176
Quarter 2	236	472	294	471
Quarter 3	236	708	294	765
Quarter 4	236	944	523	1288
Quarter 5	236	1180	300	1588
Quarter 6	236	1416	120	1708
Quarter 7	236	1652	102	1810
Quarter 8	236	1888		

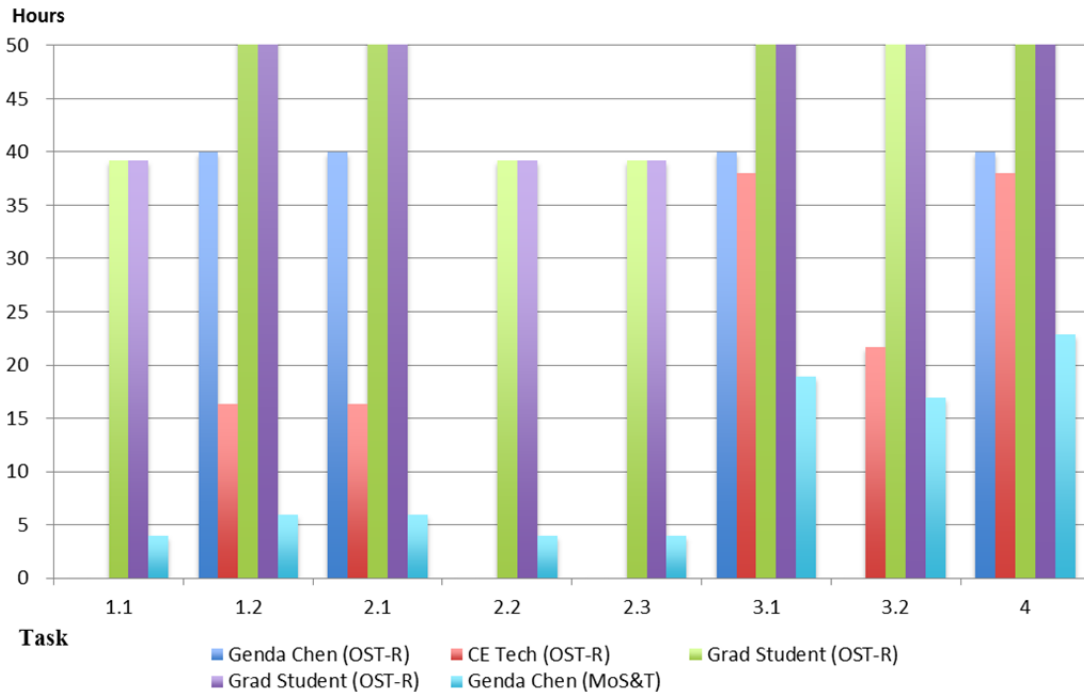


Figure 7 Cummulative Hours Spent on Various Tasks by Personnel

II.2 FUNDS EXPENDED AND COST SHARE

The budgeted and expended OST-R funds accumulated by quarter are compared in Figure 8. Approximately 92% of the proposed budget has been spent till the end of seventh quarter. The actual cumulative expenditures from OST-R, Mo S&T, and MoDOT are compared in Figure 9. The expenditure from OST-R is less than the combined amount from the Mo S&T and MoDOT, meeting the required non-federal match fund requirement.

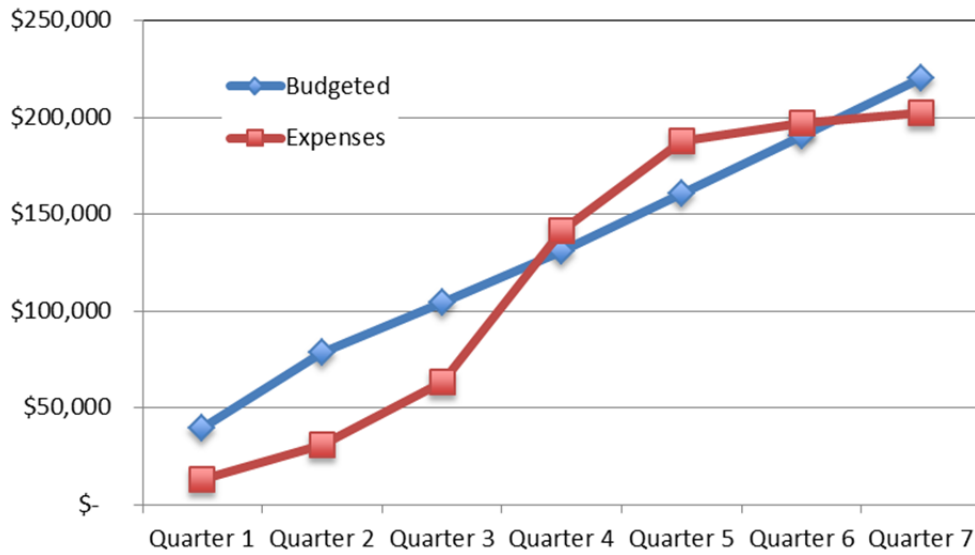


Figure 8 Comparison of OST-R Budget and Expenditure Accumulated by Quarter

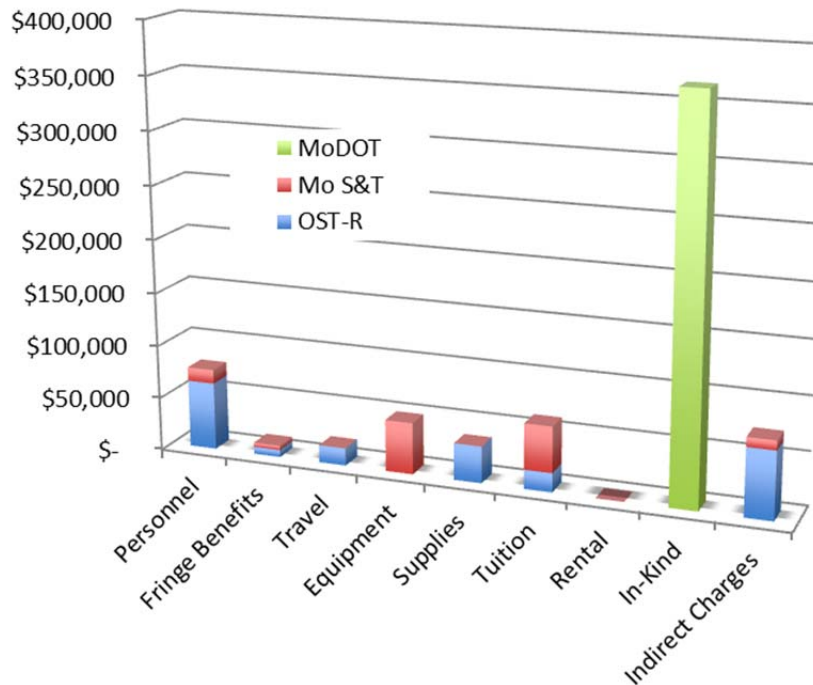


Figure 9 Cumulative Expenditures by Sponsor